

# Influence of pressure on the gel strength and on the solid-like behavior for an inverted emulsion drilling fluid

Géssica Palaoro<sup>a,\*\*</sup>, Diogo E.V. Andrade<sup>b</sup>, Jonathan F. Galdino<sup>a</sup>, Admilson T. Franco<sup>a,\*</sup>,  
Elessandre Alves<sup>c</sup>, Alex Waldmann<sup>c</sup>

<sup>a</sup> Federal University of Technology – Paraná (UTFPR) and Research Center for Rheology and Non-Newtonian Fluids - CERNN, Brazil

<sup>b</sup> Federal University of Rio Grande do Sul (UFRGS) and Rheology and Non-Newtonian Flow Laboratory – ReoSul, Brazil

<sup>c</sup> Petrobras and Leopoldo Américo Miguez de Mello Research and Development Center, Brazil

## ARTICLE INFO

### Keywords:

Inverted Emulsion  
Drilling Fluid  
High-pressure  
Rheology  
Yield Point

## ABSTRACT

Oil and gas exploration and production in deep and ultra-deep wells located in high pressure and high temperature zones (HP/HT) are increasing considerably to meet global energy demands. Exploration in HP/HT zones presents several challenges to the performance of drilling fluids to maintain wellbore stability during the drilling process. The rheological characterization of drilling fluids has been extensively investigated through experiments at atmospheric pressure; however, there are many open questions concerning high-pressure conditions. This work aims to perform a rheological characterization of inverted emulsion drilling fluid with measurements performed under a wide high-pressure range. The experiments were carried out in a rheometer coupled to the pressure cell system. The results show that the impact of the pressure is more relevant in the solid than in the liquid-like regime. Not only the viscosity, storage modulus, and yield stress tend to increase under pressure but also the material yield strain. The higher the applied pressure, the greater is the deformation that the material withstands in the solid regime. These findings can bring relevant information to the oil and gas field since the knowledge of the material gel strength under high pressures is fundamental for the drilling operation.

## 1. Introduction

The growing global demand for oil and gas has increased exploration in deep and ultra-deep wells (Lee et al., 2012; Liu et al., 2020). Deeper wells tend to exhibit a higher bottom hole pressure, above 690 bar, and temperatures above 148 °C, called high-pressure high-temperature (HP/HT) wells (Gautam et al., 2022). HP/HT conditions provide a hostile environment for the reservoir and, consequently, require an appropriate selection and formulation of the drilling fluid (Mao et al., 2020; Mitchell and Miska, 2011; Zamora et al., 2013). Oil-based drilling fluids, also known as oil-based muds (OBMs), are technically preferred and are recommended for HP/HT wells (Stamatikis et al., 2013). Several reasons support this option, including better thermal stability, better wellbore stability, and lower friction coefficients than water-based muds (WBMs) (Ibeh, 2007; Xu et al. 2013, 2014; Zhuang et al., 2018).

Drilling fluids perform essential functions such as maintaining hydrostatic pressure, transportation and suspension of drill cuttings to the

surface, cooling and lubricating the drill bit and improving wellbore stability (Xu et al. 2013, 2014; Zhuang et al., 2018). The rheological properties of the drilling fluid influence on the drilling fluid performance, as they affect parameters such as rate of penetration, hole cleaning, wellbore hydraulics and filter cake formation (Agwu et al., 2021; Gautam et al., 2022; Mohamed et al., 2021). Thus, monitoring the rheological properties of the fluid under downhole conditions is essential, since, at subsurface conditions, the properties may differ from the original values due to pressure and temperature variations that occur along the well (Agwu et al., 2021; Gautam et al., 2022; Mohamed et al., 2021). As we discuss below, the effect of pressure on the rheological behavior of drilling fluids is not well understood in the literature. The central gap in the current knowledge is the influence of pressure on the gel strength of drilling fluids.

In the last six decades, much effort had been applied to understand the effects of pressure and temperature on the rheological properties of drilling fluids (Amani, 2012; Amani and Al-jubouri, 2012; Hermoso

\* Corresponding author.

\*\* Corresponding author.

E-mail addresses: [palaorogessica@gmail.com](mailto:palaorogessica@gmail.com) (G. Palaoro), [admilson@utfpr.edu.br](mailto:admilson@utfpr.edu.br) (A.T. Franco).

<https://doi.org/10.1016/j.petrol.2022.111114>

Received 15 December 2021; Received in revised form 25 March 2022; Accepted 1 October 2022

Available online 7 October 2022

0920-4105/© 2022 Elsevier B.V. All rights reserved.

et al., 2017, 2015, 2014a, 2014b; Long et al., 2021; Rossi et al., 1999). In general, one can conclude that the apparent viscosity increased with pressure; however, it decreased with increasing temperature. It is interesting to note that many authors observed that the apparent viscosity of drilling fluids was affected by changing the temperature regardless of the pressure experienced by the fluid. On the other hand, the role of the pressure is almost negligible up to a certain pressure, which varies for each drilling fluid formulation (Alderman et al., 1988; Gandelman et al., 2007; Gokdemir et al., 2017; Herzhaft et al., 2001; Vajargah and van Oort, 2015). The increase in pressure and/or temperature experienced by the drilling fluid must provide chemical, physical, and electrochemical reactions in the material (Caenn et al., 2017; Zhuang et al., 2019). Minor changes in the chemical composition of the fluid can cause considerable differences in the rheological behavior (Zhuang et al., 2017; Caenn et al., 2017; Rodrigues et al., 2020).

One crucial role of the drilling fluids is avoiding cuttings to precipitate over the drill bit during some stoppage on the drilling process (Balhoff et al., 2011; Gautam and Guria, 2020) and to fulfill this requirement these materials develop a structured state at rest. In order to break up this gel-like structure and reach the liquid-like regime, pumping pressures higher than the usual are required to resume circulation, which can be a complex technical problem since this pressure may overcome the formation fracture pressure and damage the borehole walls. The process of breaking up the material structure is usually referred to as solid-liquid transition (Coussot et al., 2006) since the material behaves as a solid for stress below the yield stress and as a liquid when this critical stress is surpassed. The accurate determination of the behavior of the drilling fluids in this solid-like regime is essential for further understanding the solid-liquid transition and, consequently, for better choosing the strategies during the drilling process. In this scenario, the comprehension of the effects of pressure and temperature not only on the viscosity but also on the properties of the material in the solid-like regime is essential for the oil and gas industry (Maxey, 2009).

Although considerable analyzes have been developed on understanding the influence of high pressures and high temperatures on the apparent viscosity of drilling fluids, the role of these variables on the behavior of the material in the solid-like regime is still an open question. As far as we are concerned, the only attempts to study the effect of the pressure on the solid-like behavior of drilling fluids were developed by Maxey (2009) and Patel et al. (2019). In both works, the authors focused only on the influence of the frequency applied on the oscillatory test in the linear viscoelastic region for fluids with different compositions submitted to high pressures. Considering the importance of understanding the material behavior in the solid-like regime and the solid-liquid transition, the present work aims to investigate the influence of pressure on the rheological behavior of an inverted emulsion drilling fluid in three regions: liquid regime, solid regime and solid-liquid transition. The main contribution of this work is to call the community's attention that the high pressures affect not only the drilling fluid viscosity but also the material characteristics in the solid-like regime and the solid-liquid transition. The authors are not aware of a similar discussion having been reported previously. It can be anticipated that the material's gel strength is much affected by the pressure applied to this analyzed drilling fluid.

## 2. Experimental methodology

A synthetic drilling fluid kindly provided by Petrobras was selected for the experimental study. The sample is an inverted emulsion using an olefin base oil with an internal phase of sodium chloride brine, with a

60/40 oil to water ratio. Other drilling fluid components are primary and secondary emulsifiers, lime, organophilic clay, and barite.

The measurements were performed on the Anton Paar MCR 502 controlled shear stress rotational rheometer equipped with a pressure cell system that allows applying pressures up to 1000 bar. The pressure supply unit consists of an upstream hand pump that pressurizes the internal oil with a pressure range of up to 700 bar, and a spindle pump for applying pressures up to 1000 bar, and a separator unit responsible for transferring the pressure from the oil to the sample (see Fig. 1).

Fig. 1 shows the configuration of the pressure cell, the rheometer, and the pressurization unit. The pressure cell apparatus, illustrated in Fig. 2, consists of (a) magnetic coupling, which transfers the torque from the motor-drive to the internal cylinder mounted in the pressure cup; (b) pressure head that seals the cell so that it is pressure-tight; (c) measurement system, i.e., the internal cylinder; (d) pressure cup, i.e., the external cylinder from the Couette configuration. One can see under the pressure cup the connection by which the sample is pumped in the closed-cell to achieve the desired pressure before starting the rheometrical measurement.

One of the major issues in performing rheometrical measurements at high pressures is the accuracy of the measured results, especially at low shear stresses and shear rates. The sensitivity of the systems is reduced due to the torque transmission that is carried out magnetically. The results reliability was assured by performing identical protocols at atmospheric pressure using the standard configuration rheometer and the pressure cell system coupled with the rheometer. Thus, it is possible to compare both results and determine the range of shear stress and shear rate in which we can adequately analyze the fluid using the pressure cell apparatus.

The standard configuration rheometer features two separate motors, which allow rotation of the upper and/or lower geometry, with direct control of torque or rotation. We used the Couette rough surface geometry for the tests performed in the standard configuration, with 22 mm diameter for the cup, 20 mm diameter and 30 mm height for the internal cylinder. For the tests carried out with the pressure cell system, the rheometer is equipped just with one upper motor, and the bottom cup is fixed. In other words, the pressure head and the pressure cup shown in Fig. 2 are static. Consequently, the upper motor performs the control of the experiment and measurements. We also used Couette rough surface geometry in this configuration, with 30 mm diameter for the cup, 28 mm diameter and 50 mm height internal rotating cylinder.

Considering that the primary goal of the current work is to analyze the effects of pressure on the structure of the drilling fluid, all tests were performed at a constant temperature of 25 °C. The influence of higher temperatures in the drilling fluid behavior remains a topic for future work.

Rheological tests were conducted at five different pressures: atmospheric pressure, 70, 270, 500 and 800 bar. Before any test, whether in the standard configuration rheometer or with the pressure cell system, the drilling fluid sample was homogenized for 10 min on the Hamilton Beach mixer.

For tests performed with the standard configuration of the rheometer, the sample was pre-sheared for 10 min at 500 s<sup>-1</sup> and then left under a zero-shear stress condition for 10 min resting time, in which the gel development process took place. After the pre-test, the sample was submitted to different protocols: (i) measurement of the equilibrium viscosity curve in which plateaus of shear rate were applied until the steady-state shear stress determination; (ii) stress amplitude oscillatory sweep from 10<sup>-3</sup> to 100 Pa and 1 Hz; (iii) stress ramp from 10<sup>-2</sup> to 100 Pa for 5 min. For the tests performed in the rheometer coupled with the pressure cell system, the same protocol performed in the rheometer with

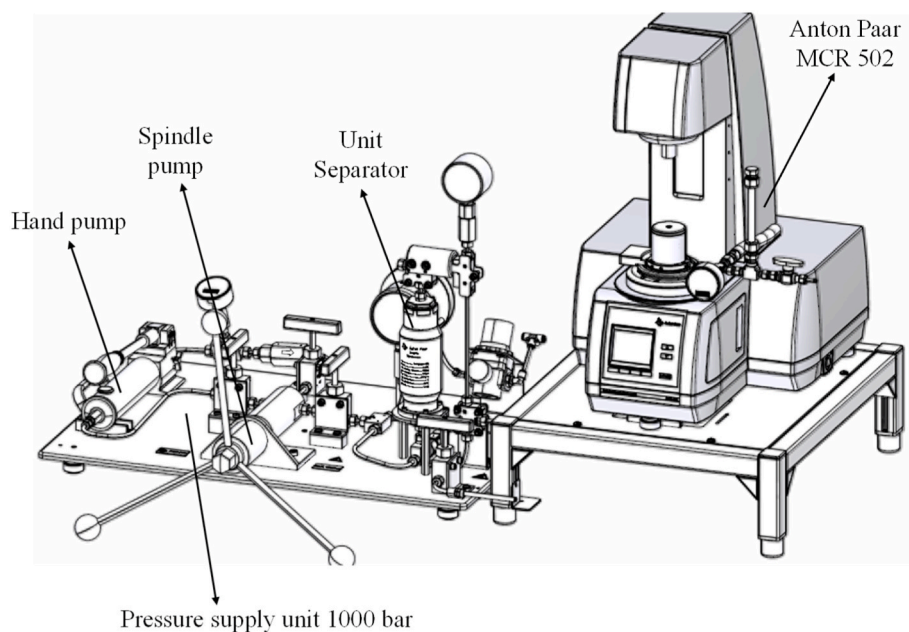


Fig. 1. Rheometer connected to the pressure cell system. Adapted from the Instruction Manual C-ETD 300/PR 1000 (2015).

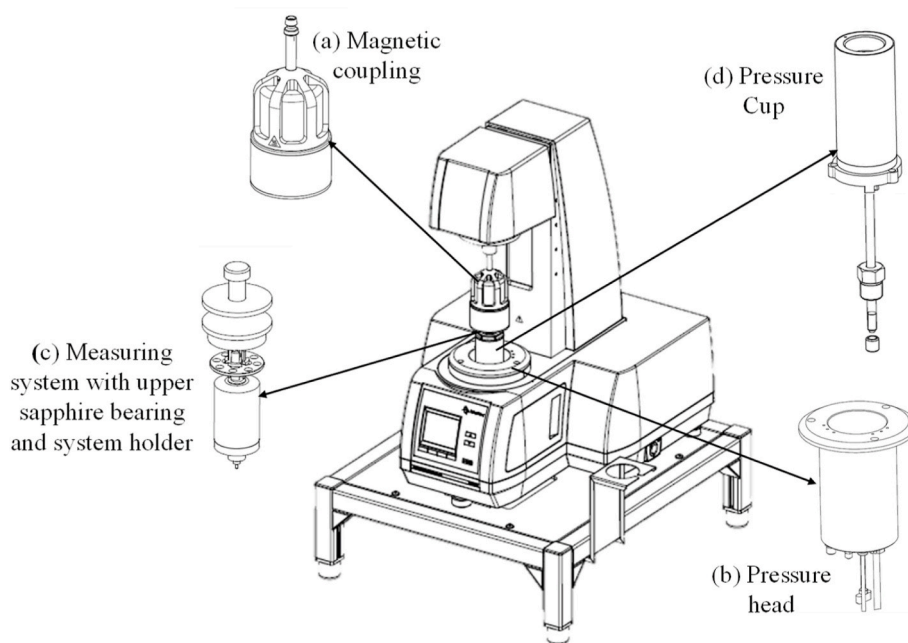


Fig. 2. Pressure cell apparatus illustration. Adapted from the Instruction Manual C-ETD 300/PR 1000 (2015).

standard configuration was followed; the only difference is that in this system, the sample is pumped into the measuring device up to the desired pressure.

### 3. Results and discussion

The influence of pressure on the rheological behavior of the drilling fluid was analyzed in three regions: the liquid-like regime, the solid-like regime, and the solid-liquid transition. First, we analyze the liquid regime. In other words, the influence of the pressure on the apparent viscosity of the material. Fig. 3 presents the material equilibrium viscosity curve under different applied pressures. In these experiments, each shear rate was imposed for enough time (minimum of 10 min) until

the material reached the steady-state for each condition. First, it is worth mentioning that the difference between the results obtained for the viscosity curve using the standard configuration (blue star) and the pressure cell (red triangle) is neglected at atmospheric pressure. We performed a single-factor statistical analysis of variance (ANOVA) with a significance level of 95% to assess the existence of any statistically significant differences between the tests performed with the usual configuration and with the pressure cell configuration at atmospheric pressure and at 25 °C. The ANOVA results are shown in the Appendix. We observed that there are no statistically significant differences between the results obtained with the usual configuration and with the pressure cell configuration.

Interestingly, it seems that as observed elsewhere (Gokdemir et al.,

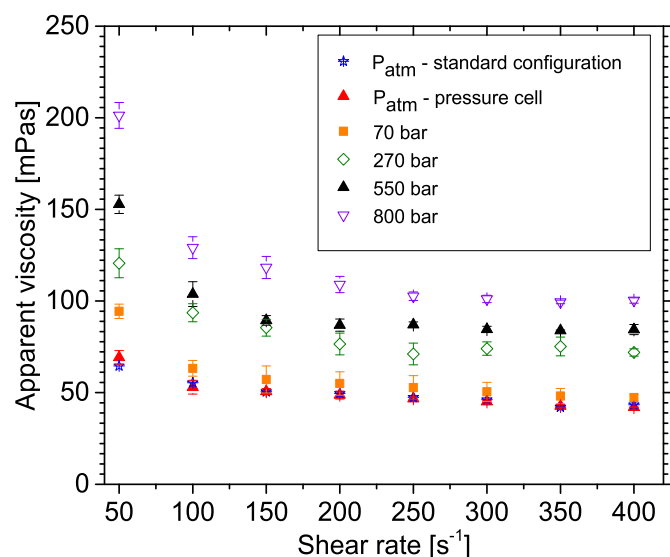


Fig. 3. Viscosity curves as a function of shear rate at 25 °C for atmospheric pressure, 70, 270, 550 and 800 bar. The experiments were repeated twice with different samples and the error bars were determined using a Student's *t* distribution with a 95.4% confidence interval as proposed by Oehlert (2010).

2017; Herzhaft et al., 2001; Ibeh, 2007; Xu et al., 2013), the effects of pressure on the viscosity are negligible up to a certain pressure level for the drilling fluid analyzed in this work. It appears that the pressure effect on the particles and droplets interactions is not enough to change the macroscopic viscosity measurement up to this value. In the current work, we observed that this pressure is between 70 and 270 bar, as shown in Fig. 3, in which, except for the lowest applied shear rate, the 70 bar pressure did not affect the fluid viscosity. It is interesting to point out that a similar range of pressure was suggested by Gokdemir et al. (2017) for another type of oil-based drilling fluid. From the pressure of 270 bar onwards, the higher the imposed pressure, the higher the viscosity (see Fig. 3). The pressure effects are most noticeable at lower shear rates; for example, the apparent viscosity measured at 50 s<sup>-1</sup> increased almost three times compared with the experiment performed at atmospheric and 800 bar-case. On the other hand, this increment was around two times for 400 s<sup>-1</sup> in this same comparison. Many researchers also observed with different oil-based drilling fluids that the apparent viscosity doubled or even fourfold when the pressure increased to values between 500 and 1000 bar, regardless of the temperature (Gandelman et al., 2007; Herzhaft et al., 2001; Torsvik et al., 2015; Vajargah and van Oort, 2015). As previously analyzed in the literature in HTHP conditions, these results show that the pressure can play a significant role in determining the operational condition since the viscosity of the drilling fluid can be much affected by the level of the well pressure during the drilling operation.

In order to verify how the pressure can modify the behavior of this drilling fluid in the solid-like regime, oscillatory stress amplitude sweep tests were performed after the pre-shear of 500 s<sup>-1</sup> and the resting time of 10 min (see Fig. 4). This protocol analyzed the storage ( $G'$ ) and dissipation ( $G''$ ) moduli as functions of the measured strain amplitude at 25 °C and different pressures applied to the sample. Three main regions can be observed in this analysis (Hyun et al., 2011):

1. The linear regime at small shear amplitudes (called SAOS – Small Amplitude Oscillatory Shear) in which the material properties are independent of the applied stress amplitude;
2. The MAOS (Medium Amplitude Oscillatory Shear) region in which some nonlinearities are observed on the measurements;
3. Finally, the material reaches the LAOS (Large Amplitude Oscillatory Shear) region, in which the nonlinearities are evident in the measurements.

In order to analyze the reliability of the oscillatory measurements using the pressure cell configuration, the comparison between the results obtained with the standard configuration rheometer (blue symbols) and the pressure cell configuration (red symbols) are shown in Fig. 4a. The figure presents the dynamic moduli ( $G'$  and  $G''$ ) on the y-axis and the stress amplitude on the auxiliary y-axis as a function of the strain amplitude. One can see that the pressure cell results can represent the main features of the curves. Some points on the curves are essential on the analysis: the values of  $G'$  and  $G''$  in the linear viscoelastic regime and mainly the comparison between both moduli that can be analyzed by the phase angle shift [ $\delta = \text{atan}(G'/G'')$ ] presented as a function of the pressure in Fig. 4f. The phase angle value can be understood as the predominance of the elastic behavior over the viscous behavior in the SAOS regime, i.e., for an elastic solid  $\delta = 0^\circ$  and a viscous fluid  $\delta = 90^\circ$  (Macosko, 1994). In addition to these characteristics on the SAOS regime, one can analyze the linear-to-nonlinear viscoelastic transition, the point at which the stress starts to impose irreversible plastic deformations in the material microstructure (Fernandes et al., 2017).

In this work, the linear-to-nonlinear viscoelastic transition strain is called a critical strain,  $\gamma_c$ , as shown by the gray arrow in Fig. 4a. It is essential to keep in mind that although one usually shows the  $G'$  and  $G''$  in MAOS and LAOS regimes and defines the yielding point in the  $G'$ - $G''$  crossover, this analysis must be carried out with caution. The dynamic moduli can just be determined appropriately in the SAOS regime (Hyun et al., 2011). The yielding behavior is further analyzed later in Fig. 5, in which a stress ramp is applied in the material, and in Fig. 6, where the values of  $G'$ - $G''$  crossover stress are analyzed. Comparing the main features in Fig. 4a, one can state that the pressure cell configuration can reliably reproduce the material's behavior in the stress amplitude oscillatory sweep. This configuration was employed to perform the experiments in the other pressures levels applied to this drilling fluid (Fig. 4b–e).

Analyzing the influence of the pressure applied on the oscillatory stress amplitude sweep (Fig. 4b–e), one can see that the greater the pressure applied, the greater the dynamic moduli. However, the increment is higher for  $G'$  than  $G''$ . Just as a comparison, the storage modulus increased one order of magnitude (from ~20 Pa to ~200 Pa), while the increment in the dissipation modulus was from ~10 Pa to ~20 Pa when the pressure increased from the atmospheric pressure (Fig. 4a) to 800 bar (Fig. 4e). The predominance of the elastic behavior over the viscous behavior as the pressure increases can be compared by the phase angle measured in the SAOS regime (Fig. 4f), i.e., the higher the applied pressure, the lower the phase angle. Table 1 summarizes the main results obtained in the rheological measurements.

As further discussed in Fig. 6, it is important to anticipate that the higher the  $G'$ , the higher the material gel strength. With this information in mind, the most exciting result in the oscillatory measurement (Fig. 4 and Table 2) is that, although the material gel strength increased with the pressure, the critical strain,  $\gamma_c$ , also increased. The increment in the pressure experienced by the fluid makes it possible to reach even greater deformations within the linear viscoelastic range of the material. This

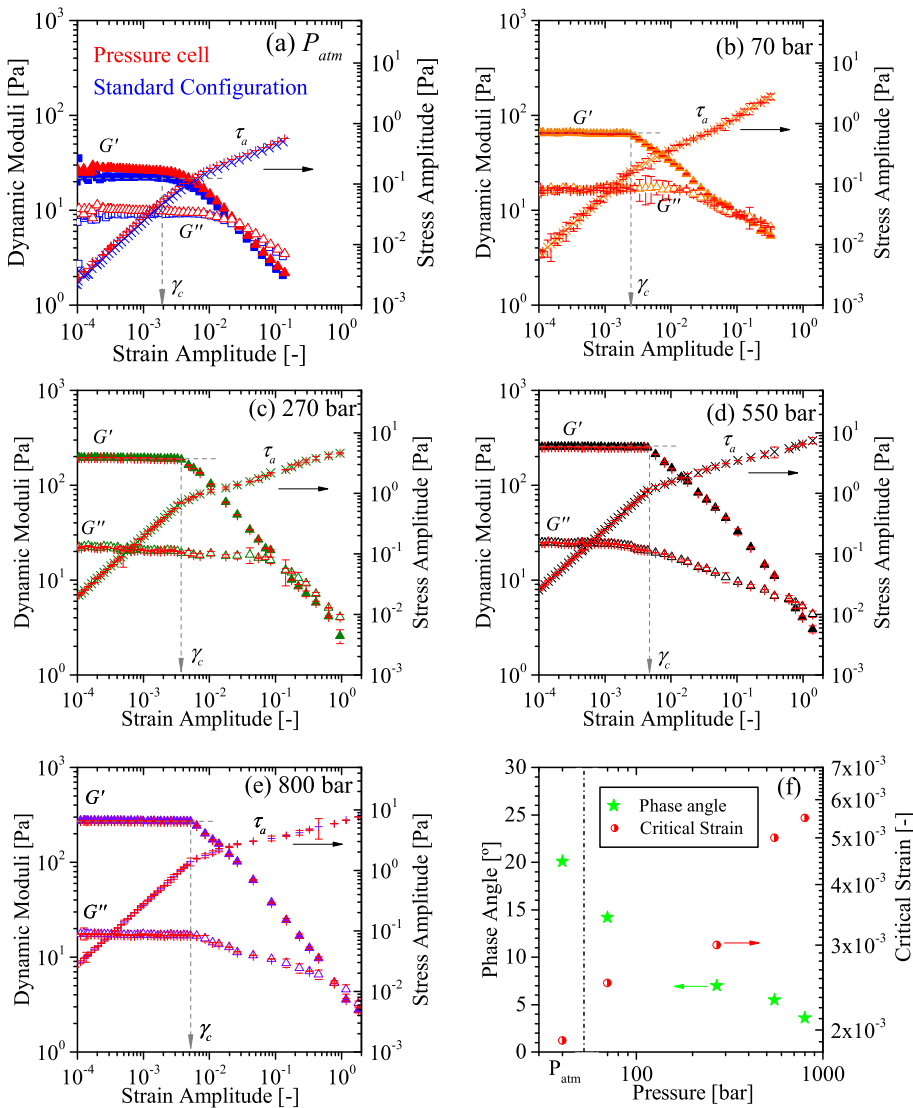


**Fig. 4.** Oscillatory stress sweep tests performed at different configurations at 1 Hz after pre-shearing the sample for 10 min at  $500 \text{ s}^{-1}$  and then left it under a zero-shear stress condition for 10 min. The experiments were repeated twice with the same sample and the error bars were determined using a Student's  $t$  distribution with a 95.4% confidence interval as proposed by [Oehlert \(2010\)](#). Figures (a)–(e) present  $G'$ ,  $G''$ , and the stress amplitude as a function of the strain amplitude of each experiment. Figure (a) presents the comparison between the measurements performed using the standard rheometer configuration (red curves) and with the pressure cell installed in the rheometer (blue curves), both at atmospheric pressure. Figures (b)–(e) show the results at different pressures applied on the sample, and figure (f) shows a compilation of the essential characteristics measured at different pressures. Experiments were performed at  $25 \text{ }^\circ\text{C}$ . (For interpretation of the references to colour in this figure legend, the reader is referred to the Web version of this article.)

linear-to-nonlinear deformation,  $\gamma_c$  is presented by the gray arrow in [Fig. 4a–e](#). A comparison between all the cases is summarized in [Fig. 4f](#), and the values are also shown in [Table 1](#).

In order to further analyze the material solid-liquid transition, unidirectional shear stress ramps were imposed on the material. In this protocol, the material behaves as a solid below the yield stress, whose strain is limited to low values. At a certain point one can see that the strain starts to increase with the applied stress rapidly; this transition can be understood as the yield point ([Andrade and Coussot, 2019](#); [N'gouamba et al., 2020](#); [Venkatesan et al., 2003](#)). [Fig. 5](#) shows the shear strain as a function of the applied stress for this protocol performed under different pressures after the same pre-shearing and resting time used in the previous analysis. First, it is essential to compare the results obtained with the standard configuration and the pressure cell. In this stress ramp, one can see that the results obtained using the pressure cell configuration reproduces quite well all the main features of the curve measured with the standard configuration. In these experiments, the yielding point was determined using the interception of two power laws fitted below and above the yielding region; for example, as

presented by the dashed line, the yield stress and strain are around 7.5 Pa and 3.1, respectively, for the 800 bar-case. It is worth emphasizing that pressure plays an essential role in the material's solid-liquid transition. Interestingly, as the pressure experienced by the fluid increases, not only does the material yield stress increase, but also one can note the increase of the material yield strain (see [Fig. 7c](#), which summarizes the influence of the pressure on the yield stress and yield strain obtained from [Fig. 5](#)).

It is worth noting that [Fernandes et al. \(2016\)](#) proposed a correlation between  $G'$  and gel strength for another oil-based drilling fluid at atmospheric pressure and different resting times. In this current work, the influence of the pressure on the storage modulus and the yield stress of this drilling fluid can be somehow correlated. Although representing different fluid characteristics ( $G'$  represents the material elasticity and the yield stress the minimum stress required to break up the material), [Fig. 6a](#) shows that both rheological parameters can also be correlated in our analyses. For the range of pressures analyzed in the current work, the higher the  $G'$ , the higher the material gel strength. Much experimental time can be saved with this information in mind since it is

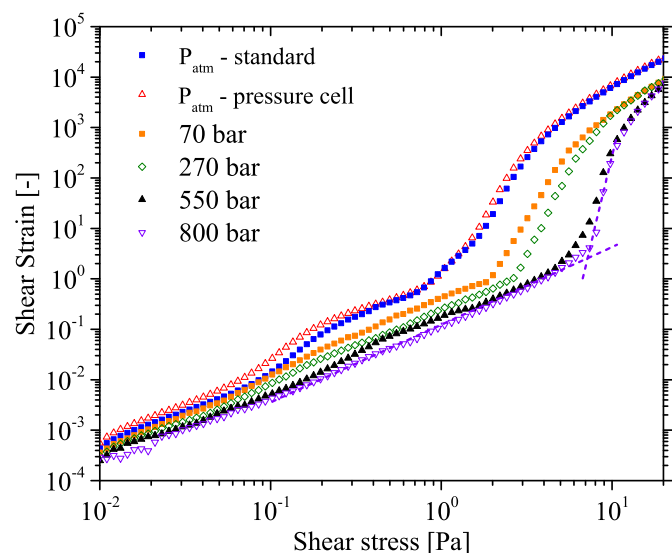


**Fig. 5.** Shear strain as a function of shear stress for a ramp of stress performed at different pressures applied on the sample at 25 °C after 10 min of pre-shearing at 500 s<sup>-1</sup> and 10 min of gel development time. The dashed lines are presented to demonstrate the procedure used to determine the yielding point.

possible to perform oscillatory measurements in the linear viscoelastic region, varying other parameters (such as the pressure applied to the fluid) without performing yielding tests in all the analyses.

Other interesting comparisons can be observed in Fig. 6b, which presents  $G'$ - $G''$  crossover stress obtained from Fig. 4 as a function of the yield stress obtained from Fig. 5. As previously discussed, although it is a standard procedure to use the  $G'$ - $G''$  crossover stress as a value to measure the gel strength, it is not indicated to use this crossover point

confidently as the material yielding point. The main reasons for this caution are that the dynamic moduli can be precisely calculated only in the SAOS region, and also the shear history imposed during the MAOS and LAOS regimes is too complex and can affect the break-up point in some materials (Andrade and Coussot, 2019). Although all these caveats, it is interesting to note that, for this material and these specific ranges of the analyzed parameters, one can recognize a correlation between the  $G'$ - $G''$  crossover stress and the yield stress presented in Fig. 6b. At least we can state that the higher the  $G'$ - $G''$  crossover stress, the higher the material gel strength.

The influence of the pressure on the liquid-like regime, solid-like regime and solid-liquid transition is summarized in Fig. 7. The rheological parameters analyzed are apparent viscosity, storage modulus and yield point. Curiously, it seems that the pressure effect is more evident in the solid-like regime (see  $G'$  in the SAOS region in Fig. 7b) and in the solid-liquid transition (yield stress in Fig. 7c) than in the liquid-like regime (see viscosity in Fig. 7a). As discussed above, the pressure in the liquid-like regime is more impacting at low shear rates; however, even for 50 s<sup>-1</sup> the apparent viscosity increased just three times compared with results at atmospheric pressure and 800 bar. Meanwhile, both  $G'$  and yield stress increased one order of magnitude at this same comparison.

Another essential point to be addressed is that the concept that the pressure affects the material only above a particular value is valid only for the liquid-regime, in which the viscosity is not much affected for the case of 70 bar applied pressure. On the other hand, the rheological characteristics are affected for the solid-like regime even for the lowest pressure imposed on the fluid (70 bar) compared with the results obtained at atmospheric pressure (see  $G'$  and the yield stress in Fig. 7). These findings bring essential information for the engineers in the oil and gas field since one of the main concerns at high pressure conditions must be the drilling fluid gel strength. In other words, under these conditions, it can be challenging to break up the material's structure and resume the flow, requiring extra care when starting the pumps.

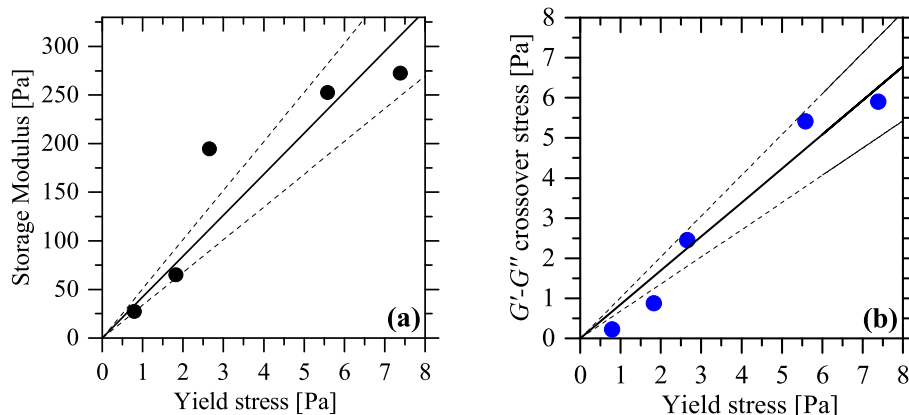


**Fig. 6.** (a) Storage modulus in the linear viscoelastic region and (b)  $G'$ - $G''$  crossover stress, both function of the yield stress. The continuous lines represent a linear relationship between the two properties analyzed with the dashed lines  $\pm 20\%$  reference.

**Table 1**

Parameter values: Storage modulus and dissipation modulus in the linear viscoelastic region; phase angle;  $G'$ - $G''$  crossover stress; critical strain obtained in oscillatory strain sweep tests and yield stress obtained in the stress ramp test at different pressures and at a constant temperature of 25 °C.

Pressure (bar)	$G'$ in the linear viscoelastic region (Pa) (Fig. 4)	$G''$ in the linear viscoelastic region (Pa) (Fig. 4)	Phase angle (°) in the SAOS region (Fig. 4f)	$G'$ - $G''$ crossover stress (Pa) (Fig. 4)	Critical strain [-] (Fig. 4)	Yield Stress (Pa) (Fig. 5)
Atmospheric	27.3	9.8	20.1	0.2	$1.90 \times 10^{-3}$	0.8
70	64.5	16.2	14.2	0.9	$2.50 \times 10^{-3}$	1.8
270	194.4	20.4	7.0	2.5	$3.00 \times 10^{-3}$	2.7
550	252.6	23.5	5.5	5.4	$5.00 \times 10^{-3}$	5.6
800	272.5	17.3	3.6	5.9	$5.50 \times 10^{-3}$	7.4

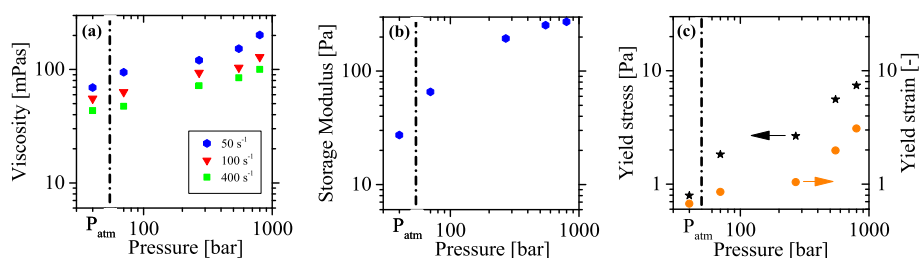


**Fig. 7.** Influence of the applied pressure on the main rheological drilling fluid parameters. (a) Liquid-like regime: Viscosity at 50, 100, and 400  $s^{-1}$ , results obtained from Fig. 3; (b) Solid-like regime: Storage modulus at the linear viscoelastic region, results obtained from Fig. 4; (c) solid-liquid transition: Yield stress and yield strain, results obtained from Fig. 5.

Finally, one can see that the same characteristics observed in the linear-to-nonlinear strain (Fig. 4f) are also noted in the material yield strain (Fig. 7c). The higher the applied pressure, the greater is the required deformation to reach the yield point for this specific drilling fluid. Therefore, we can say that pressure affects the behavior of this drilling fluid in the solid-like regime, mainly the deformation required to break up the gel. The experimental evidence to explain why pressure affects the rheological behavior of the fluid is an interesting topic for future work. Here, we can suggest a hypothesis based on ideas proposed by other researchers (Briscoe et al., 1994; Chaudemanche et al., 2009; Combs and Whitmire, 1960; Hermoso et al., 2014a, 2014b, 2015; Hiller, 1963; Maxey, 2009). The main hypothesis is that the effect of the pressure on the rheological properties of the inverted emulsion oil-based drilling fluid can be explained by the compression of the dispersed oil phase. The pressure seems to decrease the size of the emulsion droplets, affecting the interactions between the drops and the stiffness of the microstructure, promoting changes macroscopically in the mechanical response of the material.

Despite the hypothesis to explain this behavior has not been proven, the main point to be emphasized in this discussion is that the pressure experienced by the material not only affects the viscosity as reported previously in the literature but can have a significant influence on the gel strength of the drilling fluid. These results call the community's attention to analyze the effect of the pressure on the material behavior in the solid-like regime.

#### 4. Conclusions

The current work discusses the importance of analyzing the influence of high-pressure experiences by the drilling fluids not only in the liquid-like regime but also on the solid-like regime and in the solid-liquid transition. We show this discussion by investigating the effects of high pressures on the rheological behavior of an inverted emulsion drilling fluid, with a 60/40 oil/water ratio and an internal brine phase of NaCl. This analysis must be expanded for another kind of drilling fluids and other compositions in future works.

Rheological tests were performed using a pressure cell coupled to a rotational rheometer. Although the sensitivity of pressure cell-coupled rheometers was reduced, we could reproduce reliable results in the range of stress, deformation and shear rate presented in the results. We observed that pressure drastically affects the rheological behavior of the drilling fluid, with the impact of pressure being more relevant in the solid than in the liquid-like regime. The main conclusions can be summarized as:

- The inverted emulsion drilling fluid viscosity is roughly independent of the pressure up to a specific value, between 70 and 270 bar for this fluid. Above this pressure, the viscosity increased with the pressure experienced by the fluid;
- The higher the pressure applied to this fluid, the higher the storage modulus and the lower the phase angle in the linear viscoelastic

region, evidencing that higher pressures provide this fluid with a predominantly elastic behavior;

- The yield stress increased with the pressure applied to the material;
- Interestingly, the critical strain in which the material leaves the linear viscoelastic region and the yield strain increased with the pressure applied to the fluid;
- The pressure's influence is more impacting on the solid-than in the liquid-like regime since, in the analyzed range (from atmospheric pressure up to 800 bar), the apparent viscosity increased around three times while the storage modulus and the yield stress increased one order of magnitude.

These findings provide vital information for improving and managing the HP/HT well-drilling projects. The drilling engineer must have in mind that high pressures can affect not only the fluid viscosity (as pointed by other authors in previous papers) but also have a relevant impact on the gel strength of the inverted emulsion drilling fluid. In other words, the gel strength of the fluid at high-pressure conditions is underestimated if the viscometer used to determine this value operates only at atmospheric pressure. The effect of high-pressure conditions must be considered for better design and/or management of inverted emulsion drilling fluids during the start-up flow procedures.

#### Credit author statement

**Géssica Palaoro:** Conceptualization, Methodology, Validation, Formal analysis, Investigation, Writing – original draft, Visualization. **Jonathan F. Galdino:** Conceptualization, Methodology, Visualization. **Diogo E. V. Andrade:** Conceptualization, Methodology, Validation, Formal analysis, Writing – review & editing, Visualization. **Admilson T. Franco:** Writing – review & editing, Supervision, Project administration. **Elessandre A. de Souza:** Conceptualization, Supervision, Funding acquisition. **Alex T. A. Waldmann:** Conceptualization, Supervision, Funding acquisition.

#### Declaration of competing interest

The authors declare that they have no known competing financial interests or personal relationships that could have appeared to influence the work reported in this paper.

#### Acknowledgments

The authors acknowledge the financial support of PETROBRAS S/A (TC0050.0070318.11.9), CNPq(Process: 487091/2013-2), CAPES, FINEP, PRH- ANP/MCT (PRH- ANP/MCTI no. 21), and PFRH/PETROBRAS (6000.0067933.11.4 and 6000.0082166.13.4). We also thank Elis Wendt, a research engineer at the Research Center for Rheology and Non-Newtonian Fluids – CERNN, for her valuable support with the analysis of the uncertainties of the rheometric measurements.

## Nomenclature

$G'$	Storage Modulus [Pa]
$G''$	Dissipation Modulus [Pa]
$\delta$	Phase Angle [°]
$\gamma$	Strain [-]
$\tau$	Shear Stress [Pa]
$\dot{\gamma}$	Shear Rate [ $s^{-1}$ ]
HP/HT	High pressure/high temperature

## Appendix. ANOVA

We performed a single-factor statistical analysis of variance (ANOVA) with a significance level of 95% to assess any statistically significant differences between the tests performed with the standard configuration and with the pressure cell configuration at atmospheric pressure and at 25 °C. The ANOVA results are shown in Tables 2, 3, and 4 presented below.

We observed that the F parameters for all tested comparisons are lower than the critical F, indicating no statistically significant differences between the results obtained with the standard configuration and with the pressure cell configuration.

**Table 2**

ANOVA one factor to analyze significant differences in the viscosity curve performed on the rheometer with the standard configuration and with the pressure cell configuration.

Source of variation	SQ	gl	MQ	F	p-value	Fcrit
Between groups	$6.70 \times 10^{-2}$	1	$6.70 \times 10^{-2}$	$1 \times 10^{-3}$	0.975	4.60
Within the groups	903.47	14	64.53			
Total	903.54	15				

**Table 3**

ANOVA one factor to analyze significant differences in the stress amplitude oscillatory sweep tests performed on the rheometer with the standard configuration and with the pressure cell configuration.

Source of variation	SQ	gl	MQ	F	p-value	Fcrit
Between groups	268.49	1	268.49	3.45	$6.70 \times 10^{-2}$	3.97
Within the groups	5913.99	76	77.82			
Total	6182.48	77				

**Table 4**

ANOVA one factor to analyze significant differences in the stress ramp tests performed on the rheometer with the standard configuration and with the pressure cell configuration.

Source of variation	SQ	gl	MQ	F	p-value	Fcrit
Between groups	$1.44 \times 10^{-4}$	1	$1.44 \times 10^{-4}$	$1.53 \times 10^{-4}$	0.990	3.93
Within the groups	5913.99	108	0.938			
Total	6182.48	109				

## References

- Agwu, O.E., Akpabio, J.U., Ekpenyong, M.E., Inyang, U.G., Asuquo, D.E., Eyoh, I.J., Adeoye, O.S., 2021. A critical review of drilling mud rheological models. *J. Petrol. Sci. Eng.* 203 <https://doi.org/10.1016/j.petrol.2021.108659>.
- Alderman, N.J., Gavignet, A., Guillot, D., Maitland, G.C., 1988. High-temperature, high-pressure rheology of water-based muds. In: *SPE Annual Technical Conference and Exhibition*, Houston, Texas. <https://doi.org/10.2118/18035-ms>.
- Amani, M., 2012. The rheological properties of oil-based mud under high pressure and high temperature conditions. *Adv. Petrol. Explor. Dev.* 3, 21–30. <https://doi.org/10.3968/j.aped.1925543820120302.359>.
- Amani, M., Al-jubouri, M.J., 2012. An experimental investigation of the effects of ultra high pressures and temperatures on the rheological properties of water-based drilling fluids. In: *International Conference on Health, Safety and Environment in Oil and Gas Exploration and Production*, Perth, Australia. <https://doi.org/10.2118/157219-MS>.
- Andrade, D.E.V., Coussot, P., 2019. Brittle solid collapse to simple liquid for a waxy suspension. *Soft Matter* 15, 8766–8777. <https://doi.org/10.1039/c9sm01517e>.
- Balhoff, M.T., Lake, L.W., Bommer, P.M., Lewis, R.E., Weber, M.J., Calderin, J.M., 2011. Rheological and yield stress measurements of non-Newtonian fluids using a marsh funnel. *J. Petrol. Sci. Eng.* 77, 393–402. <https://doi.org/10.1016/j.petrol.2011.04.008>.
- Briscoe, B., Luckham, P., Ren, S., 1994. The properties of drilling muds at high pressures and high temperatures. *Phil. Trans. Phys. Sci. Eng.* 348, 179–207. <https://doi.org/10.1098/rsta.1994.0088>.
- Caenn, R., Darley, H.C.H., Gray, G.R., 2017. *Composition and Properties of Drilling and Completion Fluids*, Seventh. Gulf Professional Publishing, Oxford, UK.
- Chaudemanche, C., Henaut, I., Argillier, J.F., 2009. Combined effect of pressure and temperature on rheological properties of water-in-crude oil emulsions. *Appl. Rheol.* 19, 1–8. <https://doi.org/10.3933/ApplRheol-19-62210>.
- Combs, G.D., Whitmire, L.D., 1960. Capillary viscometer simulates bottom-hole conditions. *Oil Gas J.* 108–113.
- Coussot, P., Tabuteau, H., Chateau, X., Tocquer, L., Ovarlez, G., 2006. Aging and solid or liquid behavior in pastes. *J. Rheol.* 50, 975–994. <https://doi.org/10.1122/1.2337259>.
- Fernandes, R.R., Andrade, D.E.V., Franco, A.T., Negrão, C.O., 2017. The yielding and the linear-to-nonlinear viscoelastic transition of an elastoviscoplastic material. *J. Rheol.* 61, 893–903. <https://doi.org/10.1122/1.4991803>.
- Fernandes, R.R., Andrade, D.E.V., Franco, A.T., Negrão, C.O.R., 2016. Correlation between the gel-liquid transition stress and the storage modulus of an oil-based

- drilling fluid. *J. Non-Newtonian Fluid Mech.* 231, 6–10. <https://doi.org/10.1016/j.jnnfm.2016.02.003>.
- Gandelman, R.A., Leal, R.A.F., Gonçalves, J.T., Araújo, A.F.L., Lomba, R.F., Martins, A. L., 2007. Study on gelation and freezing phenomena of synthetic drilling fluids in ultradeepwater environments. In: *SPE/IADC Drilling Conference Held in Amsterdam, The Netherlands*. <https://doi.org/10.2118/105881-MS>.
- Gautam, S., Guria, C., 2020. Optimal synthesis, characterization, and performance evaluation of high-pressure high-temperature polymer-based drilling fluid: the effect of viscoelasticity on cutting transport, filtration loss, and lubricity. *SPE J.* 25, 1333–1350. <https://doi.org/10.2118/200487-PA>.
- Gautam, S., Guria, C., Rajak, V.K., 2022. A state of the art review on the performance of high-pressure and high-temperature drilling fluids: towards understanding the structure-property relationship of drilling fluid additives. *J. Petrol. Sci. Eng.* 213, 110318 <https://doi.org/10.1016/j.petrol.2022.110318>.
- Gokdemir, M.G., Erkekol, S., Dogan, H.A., 2017. Investigation of high pressure effect on drilling fluid rheology. In: *36th International Conference on Ocean, Offshore and Arctic Engineering*. <https://doi.org/10.1115/OMAE2017-61449>.
- Hermoso, J., Martínez-Boza, F., Gallegos, C., 2015. Influence of aqueous phase volume fraction, organoclay concentration and pressure on invert-emulsion oil muds rheology. *J. Ind. Eng. Chem.* 22, 341–349. <https://doi.org/10.1016/j.jiec.2014.07.028>.
- Hermoso, J., Martínez-Boza, F., Gallegos, C., 2014a. Influence of viscosity modifier nature and concentration on the viscous flow behaviour of oil-based drilling fluids at high pressure. *Appl. Clay Sci.* 87, 14–21. <https://doi.org/10.1016/j.clay.2013.10.011>.
- Hermoso, J., Martínez-Boza, F., Gallegos, C., 2014b. Combined effect of pressure and temperature on the viscous behaviour of all-oil drilling fluids. *Oil Gas Sci. Tech. – Revue d'IFP Energies nouvelles* 69, 1283–1296. <https://doi.org/10.2516/ogst/2014003>.
- Hermoso, J., Martínez-Boza, F.J., Gallegos, C., 2017. Organoclay influence on high pressure-high temperature volumetric properties of oil-based drilling fluids. *J. Petrol. Sci. Eng.* 151, 13–23. <https://doi.org/10.1016/j.petrol.2017.01.040>.
- Herzhaft, B., Peysson, Y., Isambourg, P., Delepouille, A., Toure, A., 2001. Rheological properties of drilling muds in deep offshore conditions. In: *SPE/IADC Drilling Conference Held in Amsterdam, The Netherlands*. <https://doi.org/10.2118/67736-MS>.
- Hiller, K.H., 1963. Rheological measurements on clay suspensions and drilling fluids at high temperatures and pressures. *J. Petrol. Technol.* 15, 779–788. <https://doi.org/10.2118/489-pa>.
- Hyun, K., Wilhelm, M., Klein, C.O., Cho, K.S., Nam, J.G., Ahn, K.H., Lee, S.J., Ewoldt, R. H., McKinley, G.H., 2011. A review of nonlinear oscillatory shear tests: analysis and application of large amplitude oscillatory shear (Laos). *Prog. Polym. Sci.* 36, 1697–1753. <https://doi.org/10.1016/j.propolymsci.2011.02.002>.
- Ibeh, C., 2007. Investigation on the Effects of Ultra-high Pressure and Temperature on the Rheological Properties of Oil-Based Drilling Fluids. MS Thesis. Texas A&M University.
- Lee, J., Shadravan, A., Young, S., 2012. Rheological properties of invert emulsion drilling fluid under extreme HPHT conditions. In: *IADC/SPE Drilling Conference and Exhibition, San Diego, California, USA*. <https://doi.org/10.2118/151413-MS>.
- Liu, J., Dai, Z., Xu, K., Yang, Y., Lv, K., Huang, X., Sun, J., 2020. Water-based drilling fluid containing bentonite/poly(sodium 4-styrenesulfonate) composite for ultrahigh-temperature ultradeep drilling and its field performance. *SPE J.* 25, 1193–1203. <https://doi.org/10.2118/199362-PA>.
- Long, H., Chen, W., Tan, D., Yang, L., Zhang, S., Wang, S., 2021. Development of a high temperature and high pressure oil-based drilling fluid emulsion stability tester. *Open Journal of Yangtze Oil and Gas* 6, 25–35. <https://doi.org/10.4236/ojogas.2021.62003>.
- Macosko, C.W., 1994. *Rheology Principles, Measurements and Applications*. First.
- Mao, H., Yang, Y., Zhang, H., Zhang, J., Huang, Y., 2020. A critical review of the possible effects of physical and chemical properties of subcritical water on the performance of water-based drilling fluids designed for ultra-high temperature and ultra-high pressure drilling applications. *J. Petrol. Sci. Eng.* 187, 106795 <https://doi.org/10.1016/j.petrol.2019.106795>.
- Maxey, J., 2009. Non-aqueous fluid rheology at elevated temperature and pressure. In: *National Technical Conference and Exhibition, New Orleans, Louisiana, USA*.
- Mitchell, R.F., Miska, S.Z., 2011. *Fundamentals of Drilling Engineering*, SPE Textbook Series. Society of Petroleum Engineers.
- Mohamed, A., Salehi, S., Ahmed, R., 2021. Significance and complications of drilling fluid rheology in geothermal drilling: a review. *Geothermics* 93, 102066. <https://doi.org/10.1016/j.geothermics.2021.102066>.
- N'gouamba, E., Goyon, J., Tocquer, L., Oerther, T., Coussot, P., 2020. Yielding, thixotropy, and strain stiffening of aqueous carbon black suspensions. *Journal of Rheology* 64, 955–968. <https://doi.org/10.1122/8.0000028>.
- Oehlert, G.W., 2010. *A First Course in Design and Analysis of Experiments*. Library of Congress Cataloging-in-Publication Data, USA.
- Patel, H.A., Santra, A., Thaumitz, C.J., 2019. Exceptional flat rheology using a synthetic organic-inorganic hybrid in oil-based muds under high pressure and high temperature. In: *SPE/IADC Drilling International Conference and Exhibition Held in the Hague, The Netherlands*. <https://doi.org/10.2118/194137-ms>.
- Rodrigues, R.K., Martins, S. de F.C., Naccache, M.F., de Souza Mendes, P.R., 2020. Rheological modifiers in drilling fluids. *J. Non-Newtonian Fluid Mech.* 286, 104397 <https://doi.org/10.1016/j.jnnfm.2020.104397>.
- Rossi, S., Luckham, P.F., Zhu, S., Briscoe, B.J., 1999. High-pressure/high-temperature rheology of Na<sup>+</sup>-montmorillonite clay suspensions. In: *SPE International Symposium on Oilfield Chemistry Held in Houston, Texas*. <https://doi.org/10.2118/50725-MS>.
- Stamatakis, E., Young, S., De Stefano, G., 2013. Meeting the ultrahigh-temperature/ultrahigh-pressure fluid challenge. *SPE Drill. Complet.* 28, 86–92. <https://doi.org/10.2118/153709-pa>.
- Torsvik, A., Myrseth, V., Linga, H., 2015. Drilling fluid rheology at challenging drilling conditions - an experimental study using a 1000 bar pressure cell. *Ann. Transact. Nordic Rheol. Soc.* 23, 13–20.
- Vajargah, A.K., van Oort, E., 2015. Determination of drilling fluid rheology under downhole conditions by using real-time distributed pressure data. *J. Nat. Gas Sci. Eng.* 24, 400–411. <https://doi.org/10.1016/j.jngse.2015.04.004>.
- Venkatesan, R., Östlund, J.A., Chawla, H., Wattana, P., Nydén, M., Fogler, H.S., 2003. The effect of asphaltenes on the gelation of waxy oils. *Energy Fuel* 17, 1630–1640. <https://doi.org/10.1021/ef034013k>.
- Xu, L., Chuan, S., Xu, M.B., Zhao, L., Wen, S.C., Liu, W.H., Xu, J., You, F.C., Gong, C., 2014. Experimental investigations into the performance of a flat-rheology water-based drilling fluid. *SPE J.* 19, 69–77. <https://doi.org/10.2118/163107-pa>.
- Xu, L., Zhao, L., Xu, M.B., Xu, J., Wang, X., 2013. Lab investigations into high temperature high pressure rheology of water-based drilling fluid. *Appl. Mech. Mater.* 418, 191–195. <https://doi.org/10.4028/www.scientific.net/amm.418.191>.
- Zamora, M., Roy, S., Slater, K., Troncoso, J., 2013. Study on the volumetric behavior of base oils, brines, and drilling fluids under extreme temperatures and pressures. *SPE Drill. Complet.* 28, 278–288. <https://doi.org/10.2118/160029-PA>.
- Zhuang, G., Jiang, W., Zhang, Z., 2019. Organic modifiers of organo-montmorillonite in oil system under high temperatures: desorption or degradation? *Ind. Eng. Chem. Res.* 58, 2644–2653. <https://doi.org/10.1021/acs.iecr.8b05915>.
- Zhuang, G., Zhang, Z., Jaber, M., Gao, J., Peng, S., 2017. Comparative study on the structures and properties of organo-montmorillonite and organo-palygorskite in oil-based drilling fluids. *J. Ind. Eng. Chem.* <https://doi.org/10.1016/j.jiec.2017.07.017>. The Korean Society of Industrial and Engineering Chemistry.
- Zhuang, G., Zhang, Z., Peng, S., Gao, J., Jaber, M., 2018. Enhancing the rheological properties and thermal stability of oil-based drilling fluids by synergetic use of organo-montmorillonite and organo-sepiolite. *Appl. Clay Sci.* 161, 505–512. <https://doi.org/10.1016/j.clay.2018.05.018>.